OPEN FORUM

Cosmetic Medicine

The Superior Effect of Radiofrequency With Targeted Ultrasound for Facial Rejuvenation by Inducing Hyaluronic Acid Synthesis: A Pilot Preclinical Study

Diane Duncan, MD, FACS; Jan Bernardy, PhD; Nikola Hodkovicova, PhD, PharmD; Josef Masek, PhD, MS; Marketa Prochazkova, PhD, MSc; and Rea Jarosova, PhD

Aesthetic Surgery Journal Open Forum 2024, 1–8

https://doi.org/10.1093/asjof/ojae005
www.asjopenforum.com

OXFORD UNIVERSITY PRESS

Abstract

Background: The level of dermal hyaluronic acid (HA) can be depleted by 75% at age 70. HA provides dermal hydration, volume, and thickness, making it a major component of the extracellular matrix. Restoration of dermal and epidermal HA can be achieved by combining radiofrequency (RF) energy and targeted ultrasound (TUS). The monopolar RF generates heat, with the TUS stimulating HA production. The heat induces a regenerative response in the skin, increasing the fibroblast activity and producing various extracellular matrix compounds, including HA.

Objectives: To investigate the effect of the simultaneous application of RF + TUS or RF + US on the stimulation of HA production.

Methods: Twelve animals underwent 4 treatments. Six were treated with transcutaneous RF + TUS and 6 with the combination RF + US. The opposite untreated side served as a control. Punch biopsies of the skin were taken at baseline, immediately posttreatment, 1 month, and 2 months posttreatment. The tissue was evaluated with real-time quantitative polymerase chain reaction (RT-qPCR), matrix-assisted laser desorption (MALDI) and time of flight (TOF), and confocal microscopy.

Results: The RT-qPCR focused on assessing the production of *has1* and *has2*, enzymes responsible for HA synthesis. RT-qPCR results of the RF + TUS group revealed a +98% and +45% increase in hyaluronic synthetase (HAS) 1 and HAS2 production after the treatments, respectively. The MALDI–TOF revealed a +224% increase in measured HA 2 months after the treatments. The changes were also visible in the confocal microscopy. The control group showed no significant ($P > .05$) results in either of the evaluation methods.

Conclusions: Concurrent application of RF and TUS significantly enhances the natural regenerative processes in skin tissue.

Level of Evidence: 5

Editorial Decision date: January 11, 2024; online publish-ahead-of-print January 30, 2024.

Dr Duncan is a plastic surgeon in private practice in Fort Collins, CO, USA. Drs Bernardy, Hodkovicova, Masek, and Jarosova are clinical researchers, Veterinary Research Institute, Brno, Czechia.
Dr Prochazkova is a researcher, Department of Chemistry, Faculty of Science, Masaryk University, Brno, Czechia.

Corresponding Author:
Dr Diane Duncan, 1701 East Prospect Road, Fort Collins, CO 80525, USA.
E-mail: momsurg@aol.com; Instagram: @drdianeduncan

The skin mirrors our age, and therefore, the major feature of the antiaging process is skin rejuvenation. The intrinsic and extrinsic processes of skin aging share similar molecular mechanisms, such as the reactive oxygen species that are involved in both processes and affect the ability of fibroblasts to produce all components of the extracellular matrix (ECM), therefore enhancing the signs of aging.[1] The first sign of aging may be caused by the absence of hyaluronic acid (HA) instead of changes in collagen and elastin.[2] HA is the major glycosaminoglycan present in the human skin and the key contributor to moisture retention. It creates an interface between collagen and elastin fiber and thus fills the ECM, improves mechanical support in the skin, and scavenges free radicals.[1] With sufficient levels of HA, the skin is healthy, elastic, filled, and retains a young appearance, but HA is constantly being turned over in the body and degraded inside the lysosomes by hyaluronidases encoded by *hyal1* and *hyal2* genes.[3-6]

The depletion of hyaluronic is currently treated by rejuvenating-rich moisturizers, wrinkle creams, or injections containing HA, and vitamins. These methods directly deliver HA or vitamins in the skin tissue and substitute the function of fibroblasts, but are unable to restore the body's natural ability to produce HA. Radiofrequency (RF) and ultrasound (US) energies were used, aiming to restore the synthesis of HA, yet, as standalone procedures were "only" found to stimulate the production of collagen and elastine.[2,7]

A novel technology simultaneously emits monopolar RF and targeted US (TUS) to utilize the benefits of synergistic effects of both technologies when applied simultaneously. RF causes the temperature to increase by oscillating electrical current to the treated tissue, where it drives collisions between charged molecules and ions, converting this kinetic energy into heat, while US is a mechanical compression wave that stimulates the tissue through both mechanical and thermal mechanisms.[8,9] Although both modalities contribute in providing heat and mechanical stress, TUS is focused similar to the way magnifying glass focuses light, creating a smaller yet concentrated area of effect that allows for deeper and more accurate targeting. This enables higher temperatures without causing undesired effects within the reticular dermis, the location with the most active dermal fibroblasts.[9-11] These are mechanically stimulated, leading to additional thermal increments and mild intracellular vibrations in this layer.

It is hypothesized that combining the thermal and mechanical stress of the fibroblasts may trigger processes that may not lead only to enhanced collagen and elastin production but may actually boost the natural synthesis of HA as well.

This study aims to determine the effects of the simultaneous use of RF and TUS treatment on the production of HA and the importance of targeting the energy to the reticular dermis for the best possible outcomes. Thus, the study will compare the technology combining RF with TUS with a technology combining RF with general non-TUS.

METHODS

This investigational, single-center, 2-arm animal study was approved by the Institutional Animal Care and Use Committee and the Ethics Committee for Animal Protection of the Ministry of Agriculture. The study took place between June and October 2020. It was supervised and performed by the Veterinary Research Institute (VRI, Brno, CZ), a holder of the Good TUSultrLaboratory Practice Authorisation. Animals were stabled at the VRI during the study duration, with the certified veterinarian and veterinary staff handling the animal care to secure animal well-being.

Twelve sows (*Sus scrofa f. domestica*, 60-80 kg) were divided into 2 groups. Both groups underwent four 20 min treatments 2 to 3 days apart delivered to the abdomen. The treatment area was approximately 25 cm^2. One group ($n = 6$) was treated with a small applicator that simultaneously emits RF and TUS (Exion, BTL Industries Inc., Boston, MA), with the second ($n = 6$) treated with RF and non-TUS (BTL Exilis System, BTL Industries Inc. Boston, MA). All utilized energies were set to 100%. The untreated side of the abdomen served as a control.

Animals were kept under general anesthesia during the treatment procedure and sample collection. The anesthetic (Propofol 2% MCT/LCT Fresenius, dosing 1-2 mg/kg) was delivered to the pig's system by an intravascular cannula placed into the ear's vein. All animals were preventively intubated and monitored by electrocardiogram (EKG) with a certified veterinarian overseeing the vital signs, together with assessing study-related adverse events and side effects. The animals were euthanized by an analgesic overdose (T61 a.u.v. inj., Intervet International B.V./MSD AH) administered by a veterinarian after the study completion.

Six tissue samples (3 from the treated side and 3 from the untreated side) were taken by a 6 mm punch biopsy needle at baseline, after the last treatment, and 1 and 2 months after the last treatment. Overall, 252 samples were taken and used for analysis. Upon the biopsy extraction, the sample site was numbed by injecting local anesthetic (Lidocaine 2% a.u.v. inj., Fatro s.p.a., dosing 2 mL per biopsy) to relieve the pain upon waking up. The sampling wound was disinfected, enclosed by 2 clamps, and covered by an Aluminium Silver Spray Skin Care.

The effect of the procedures was evaluated by real-time quantitative polymerase chain reaction (RT-qPCR), mass spectrometry separation technique based on molecular weight (MW) using matrix-assisted laser desorption (MALDI) in combination with a time-of-flight (TOF) analyzer, and Confocal microscopy. RT-qPCR is a very sensitive

technique that allows the amplification of a specific segment of DNA and makes copies of DNA fragments or genes, which allows the identification and quantification by size and charge of gene sequences using visual techniques.[12] To support the data obtained by RT-qPCR analysis, the HA within the skin tissue was evaluated using the MALDI–TOF method, which is an analytical method that reflects the presence and amount of HA in the organism based on its MW.[13,14] Confocal microscopy is a broadly used visualization technique to resolve the detailed structure of specific objects. Various components of cells or tissue sections can be specifically labeled using immunofluorescence. HA is visualized by green color and the cell nucleus by blue color.[15]

RT-qPCR Analysis

Skin tissue samples were fixed in RNA later (Thermo Fisher Scientific, Waltham, MA), left for 24 h at 4°C, and then stored at −80°C until RNA extraction.

Skin tissue samples were individually removed from RNAlater, dried, cut into smaller pieces with sterile scissors, and homogenized on the MagNaLyser (Roche, Basel, Switzerland) in 0.75 mL of TRI Reagent RT (Molecular Research Center, Cincinnati, OH). Total RNA free of DNA contamination was further purified using the RNeasy Mini kit (Qiagen, Hilden, Germany) according to the manufacturer's protocol. According to the manufacturer's instructions, the RNA was reversely transcribed to messenger RNA using the LunaScript RT SuperMix Kit (New England BioLabs Inc., Ipswich, MA). The individual sample RNA was diluted with RNase-free water (Qiagen, Hilden, Germany) to obtain the same resulting RNA concentration for all samples, that is, 1 μg. The control samples were included and prepared as recommended by the manufacturer. The resulting 20 μL reaction was heated at 25°C for 2 min to ensure primer annealing, followed by 55°C for 10 min when the complementary DNA (cDNA) was synthesized and the reaction was inactivated by 95°C for 1 min. For reverse transcription, the Engine Thermal Cycler (Bio-Rad, Hercules, CA) tool was used. The samples of cDNA, including the controls, were stored at −20°C until RT-qPCR, which can record the amount of DNA throughout the cycle, was performed.

Biopsy samples were evaluated by molecular biochemistry through gene expression of markers that are involved in HA production processes such as *tgfb1*, *fgf1*, *has1*, *has2*, *has3*, and membrane receptor *cd44*. Hyaluronan synthases (HASs) are enzymes synthesizing molecules of HA, there are 3 types of HAS based on the molecular dimension of synthesized molecules of HA—HAS1, HAS2, and HAS3.[5,16] HAS2 synthesized large-size molecules of HA (2×10^6 Da); therefore, it plays a major role in the syntheses of HA in fibroblasts, myofibroblasts, and most importantly in the dermis itself,[3,17] while HAS1 facilitates the formation of both large and small molecules, synthesized by HAS3.[17-19] Transforming growth factor beta 1 (TGF-β1) is a major regulator of biosynthesis in the ECM, throughout the activation of signaling pathways that regulate ECM genes and induce collagen, fibronectin, and elastin production in the dermis.[1] TGF-β signaling pathway is essential for maintaining structural and mechanical integration of dermal connective tissue by increasing ECM production. TGF-β1 controls proliferation and cell differentiation.[1,7,20] An acidic fibroblast growth factor 1 (FGF1) plays a role in the regeneration and proliferation of fibroblast cells, which produce collagen and elastin, and leads to HAS expression and synthesis of HA.[19,20] CD44 is a major receptor for HA.[5] After the interaction with HA, several biological processes are activated such as endocytosis, cell migration, differentiation (specialization), and proliferation (cell formation).[16] HA in conjunction with CD44 supports skin tightening, hydration, and elasticity. CD44 also regulates the expression of proteins based on corneocyte and keratinocyte differentiation, so it might be assumed that the treatment may target not only the dermis but also, to some extent, epidermis as well.[17]

Sequences for primers were designed using the NCBI primer-blast design tool available online. The obtained data were analyzed using the LightCycler 480 SW 1.5 program (Roche, Basel, Switzerland) within the comparative 2Δ threshold cycle (Ct) method. The HPRT gene was chosen as an optimal reference gene for data normalization using the NormFinder software (MOMA, Aarhus, Denmark). The relative expression was calculated according to the formula: [1/(2Ct of gene)]/[1/(2Ct HPRT)].[21] In each run, cycling conditions were as follows: initial denaturation at 95°C for 15 min; 45 cycles of denaturation at 95°C for 15 s, primer annealing at 58°C for 30 s, and extension at 72°C for 30 s. Melting analysis was performed at 60 to 95°C.

Matrix-Assisted Laser Desorption Time of Flight (MALDI–TOF)

A novel application of MALDI–TOF MS Autoflex speed (Bruker Daltonics, Billerica, Massachusetts) was used in positive linear mode with laser energy of 80%, frequency of 2000 Hz, and a sum of spectra 10,000. Calibration of the MS instrument was done with Protein standard II in the range of 20 to 80 kDa with extrapolation for higher masses. 2,5-Dihydroxybenzoic acid, a saturated solution in organic solvent (MeCN with 1% trifluoroacetic acid), was used as a matrix. Samples for measurement were prepared by extraction to acetone, 0.5 M NaCl, and ethanol.

Samples tissues were put to the 0.5 mL of acetone and left in solution in 1.5 mL Eppendorf tube overnight (for tissue breakdown). After 24 h acetone was removed and samples of tissues were put into the 0.25 mL of 0.5 M NaCl aq. solution and shook in a 1.5 mL Eppendorf tube in the shaker at 800 rpm for 2 h. Samples of tissues were removed and put into the mixture of glycerol and 0.5 M

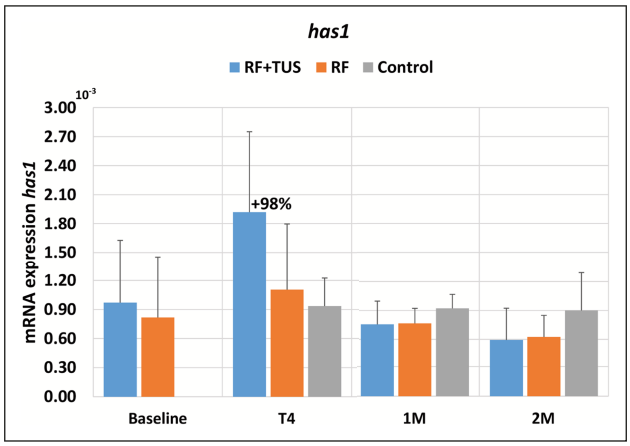

Figure 1. The bar chart of *has1* concentration evaluated by real-time quantitative polymerase chain reaction. 1M, 1-month follow-up; 2M, 2-month follow-up; RF, radiofrequency; energy; T4, last (fourth) treatment; TUS, targeted ultrasound.

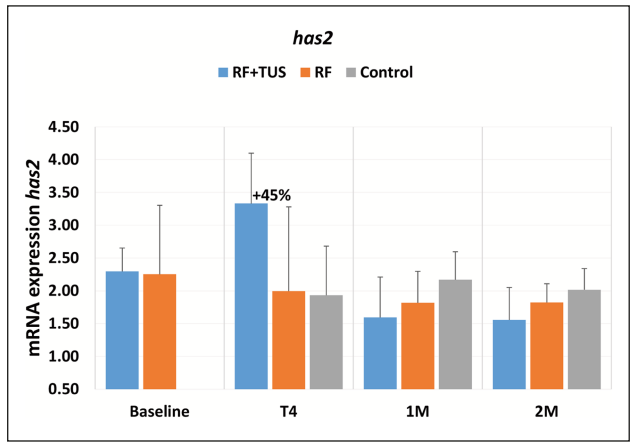

Figure 2. The bar chart of *has2* concentration evaluated by real-time quantitative polymerase chain reaction. 1M, 1-month follow-up; 2M, 2-month follow-up; RF, radiofrequency; energy; T4, last (fourth) treatment; TUS, targeted ultrasound.

NaCl aq. (v/v, 1:1) and put in the freezer (−40°C) for keeping and the possibility of next usage. Sample extracts were mixed with ethanol in the range sample extract/ethanol, v:v, 1:5. It means mixing the 0.25 mL of the sample extract in 0.5 M NaCl aq. solution with 1 mL of ethanol. Immediately after mixing samples with ethanol, extracts were put in the fridge and left at 7°C for 16 h (for the formation of a precipitate of the HA and its separation from the lower molecular proteins). Sample precipitates were centrifuged at 14,000 rpm for 20 min, after centrifugation, the supernatant was removed, and the precipitates were completely dissolved in 100 µL of ultrapure water. After the dissolution of the precipitates, 75 µL of ethanol were added to each sample (for the precipitation of the high-molecular proteins). Samples were then centrifuged at 14,000 rpm for 20 min, and surfactants were used for MALDI–TOF MS measurements. Then, a direct application of each sample to the plate and dripping of the matrix were proved immediately before MALDI–TOF measurement.

Confocal Microscopy

Each collected sample was vertically cut into 5 µm thick slices, then fixated in a fixative consisting of 3.7% formaldehyde-PBS, 70% ethanol, and 5% glacial acetic acid. A 1:100 dilution of biotinylated hyaluronan-binding protein solution was used to bond with HA and was left to incubate for 12 to 16 h in 4°C. After the incubation, slides carrying the samples were washed, stained with streptavidin conjugated with a fluorescent label (Alexa 488), and left to incubate for 1 h in the dark. Samples were then washed again and to mount, VectaShield with DAPI (Vector Laboratories, Newark, CA) was used. The samples were sealed with nail polish around the edges of the coverslip. The images of the prepared samples were conducted through Leica Microsystem, LAS X 3.5.1.18803 (Wetzlar, Germany), at a wavelength of 580 nm and magnification of 63×. Protocol from the National Heart, Lund and Blood Institute under award number PO1HL107147 inspired this process.[22]

Statistical Analysis

The statistical analysis was done by using the Real Statistics Resource Pack software for Microsoft Excel.[23] The difference between the individual measurements was tested by the Friedman test. The significance level α was set at 5%.

RESULTS

All 12 animals underwent 4 treatments and collection of samples at baseline, after the treatment, 1-month, and 2-month follow-up visits. The 252 collected samples were divided into 3 groups, 1 for each evaluation method with a control. The control samples were evaluated together regardless of group.

RT-qPCR Results

RF + TUS

The production of *has1* and *has2* peaked after the treatment, with *has1* and *has2* showing a 98% and 45% increase ($P < .001$), respectively. The production of *has1* and *has2* slowly decreased at 1-month and 2-month follow-ups. *has3* production peaked at a 1-month follow-up with an 85% increase, and similarly to *has1* and *has2*, the value measured at a 2-month follow-up slightly decreased. The *fgf1* and *fgfb1* peaked at 1-month follow-up with a 113%

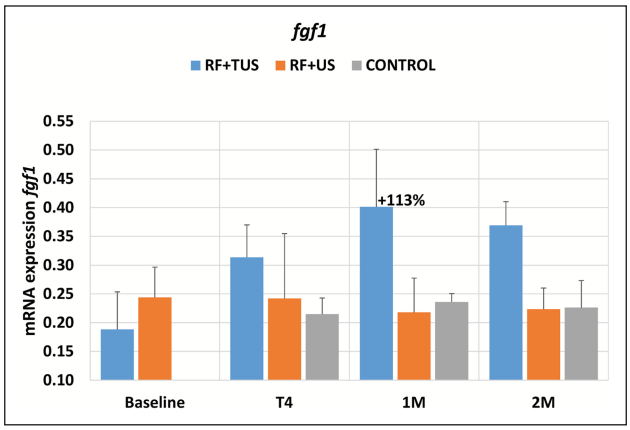

Figure 3. The bar chart of *fgf1* concentration evaluated by real-time quantitative polymerase chain reaction. 1M, 1-month follow-up; 2M, 2-month follow-up; RF, radiofrequency; energy; T4, last (fourth) treatment; TUS, targeted ultrasound.

and 31% increase ($P < .001$), respectively. The last measured marker, the receptor *cd44* for HA peaked at a 2-month follow-up with a 27% increase. Figures 1-3 represent a graphical visualization of the changes.

RF + US and Control

The RT-qPCR evaluation discovered no change in the measured parameters in Group B or in the control samples.

MALDI–TOF

The analysis of the MW of molecules in the samples showed a peak between 66 and 68 kDa, which corresponds with the MW of HA, due to the extrapolation for higher masses.

RF + TUS

Based on the MALDI–TOF evaluation, the amount of HA in the sample showed a gradual increase by 79% at the 1-month follow-up and by 224% at the 2-month follow-up ($P = .022$).

RF + US and Control

Group B showed no clear trend in the HA changes as the results fluctuated between 14% at the 1-month follow-up, and 11% at the 3-month follow-up when compared with baseline. However, those changes were not statistically significant in either Group B ($P = .1353$) or the control group ($P = .3173$).

Confocal Microscopy

After the marker-detecting techniques, the presence of HA was visualized through confocal microscopy. Figure 4 shows the different intensities of colors representing HA (green) and cell nucleus (blue), where the top row (A-D) represents RF + TUS, while the bottom row (E-H) represents RF + US. The apparent intensification of the color green in the samples shows the continuous improvement in the production of HA in the RF + TUS group while showing no change in the RF + US group. The pictures of the RF + TUS group show deeper and more lasting HA production. The green color appears brighter in the epidermis, where the keratinocytes are densely placed and produce the HA, while in the dermis, HA is produced by fibroblasts, which are separated by an ECM and collagen fibers, and the brightness seemingly fades.

DISCUSSION

This present study aimed to compare the technology combining RF with TUS with a technology combining RF and general non- TUS in their ability to alter the natural processes leading to the synthesis of HA in the skin. The obtained data documented the changes occurring in the skin of 12 sows 2 months after receiving four 20 min treatments. No study-related adverse events or side effects were observed in the animals or samples obtained.

Approximately, 50% of the body's deposit of HA is located in the skin.[24] HA is an extremely hydrophilic molecule that is able to retain up to 100 times its weight in water[25] with a very dynamic turnover of approximately 24 h. In lower HA concentrations, the turnover is accelerated.[26] Apart from moisture retention, HA functions in the framework for blood vessel formation and the framework through which cells migrate, wound healing, and tissue repair.[27] HA also has the ability to stretch the fibroblasts and stimulate collagen and tubulin production.[28,29] As the variability of HA use in the body is so vast, reminding the dermal fibroblasts of HA production may improve the skin's overall health.

The presented study provided novel information on the noninvasive stimulation of HA production, as both quantification and visualization methods indicate the superior results of the simultaneous application of RF + TUS to RF + US. All of the methods demonstrated highly significant changes ($P < .001$) in the RF + TUS group, while no statistically significant changes ($P > .05$) were observed in the RF + US group or the control, indicating the importance of stimulating the deep dermal layer reachable only by the TUS.

Fibroblasts, under specific circumstances, can initiate increased elastin production contingent upon the presence of sufficient TGF-β and FGF.[30] Moreover, in response to certain external conditions, fibroblasts may engage in the production of HA, involving a complex biosynthetic cascade orchestrated by various enzymes and cofactors such as TGF-β, epidermal growth factor, and platelet-derived growth factor.[31] We hypothesize that the mentioned impact of heat and mechanical stress on

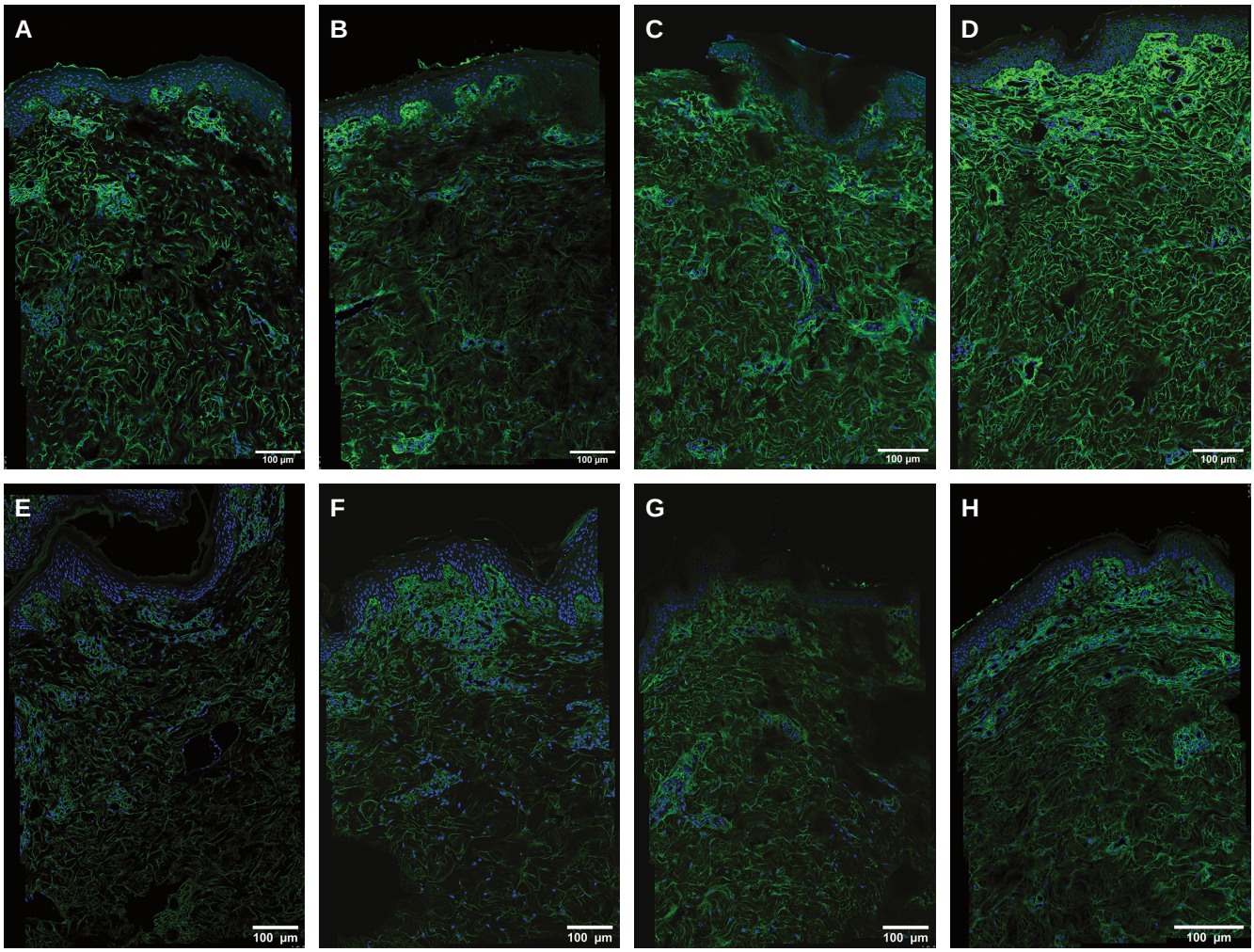

Figure 4. The visualization of hyaluronic acid through confocal microscope, magnification of 63×, radiofrequency (RF) + targeted ultrasound (TUS): (A) baseline, (B) after the last treatment, (C) 1-month follow-up, (D) 2-month follow-up; RF + US: (E) baseline, (F) after the last treatment, (G) 1-month follow-up, (H) 2-month follow-up.

fibroblast metabolism contributes to this cascade, creating favorable conditions for HA synthesis.

First, the samples were proceeded by RT-qPCR analysis which revealed the changes connected to the RF + TUS therapy. Immediately after the treatments, the expression of genes for enzymes synthesizing the HA peaked (*has1* + 98%, *has2* + 45%), with the last enzyme peaking at a 1-month follow-up (*has3* + 85%). This has been followed by a subsequent decrease in the synthases levels, most likely due to the negative feedback regulation of enzymes, where the product limits its production when reaching a certain amount and aims to restore homeostasis after enough HA-synthesizing enzymes were produced,[32] leading to increased production of *tgfb1* gene, which is an ECM biosynthesis regulator (+31% at 1-month follow-up). HA also influences the fibroblast proliferation[33]; therefore, the increase in HA leads to an increase in *fgf1*, a fibroblast growth factor, production (+113% at 1-month follow-up). The last measured marker, *cd44*, a membrane receptor, showed a gradual increase as it was adapting to the increasing amount of HA in the skin while peaking 2 months after the treatments (+27%). After the RT-qPCR evaluation, which measured genes involved in HA or fibroblast production and interaction, MALDI–TOF measured the amount of HA in the sample. The amount of HA peaked at the 2-month follow-up which represented an increase of +224%. As all 3 HASs were activated, we can assume that HA of all MW was synthesized. However, the most detected HA in the sample is low-molecular-weight (LMW) HA, which is depolymerized from high MW HA.[34] LMWHA is an important molecule that is biologically active and affects cellular behavior, including wound care, fibroblast, and endothelial cell migration and activation.[34] The prevailing presence of LMWHA may be one of the reasons for such a complex ECM response.

These results of quantification methods are supported by the confocal microscopy pictures, which visualized the increased amount of HA in the skin after the RF + TUS, which filled the ECM (Figure 4).

The first limitation of this study is the sample size; although even with 6 animal cases per group, the statistical analysis found significance in the observed markers. Due to the physiological similarities between pig and human skin, in addition to the invasive nature of sample collection, we believe that the use of an animal model was necessary and an adequate first step into acquiring insights into this previously undescribed phenomenon. However, a small sample size poses limitations to statistical analysis and its potency. In order to minimize the stress induced on animals, the last sample was obtained 2 months posttreatment. In order to verify the efficacy of these findings, the study warrants a longer follow-up as well as advancement to human trials in a statistically meaningful population.

CONCLUSIONS

This pilot animal histology study suggests that the simultaneous use of RF + TUS treatment is able to enhance the natural production of HA through stimulation of fibroblasts, while RF + US treatment is not. If confirmed by further studies, this method could present a shift in the rejuvenation field as it restores the cells ability to produce the major skin components. As such this could become a viable tool for facial rejuvenation.

Disclosures

Drs Duncan and Bernardy are consultants for BTL (Boston, MA). Drs Hodkovicova, Masek, and Prochazkova are associates of VRI. All authors declared no potential conflicts of interest with respect to the research, authorship, and publication of this article.

Funding

BTL Industries (Boston, Mass) was the sponsor of this study and provided the study device. However, no funding for authorship or publication of this article was provided. The authors thank the Ministry of agriculture of the Czech Republic for Institutional Support No. MZE-RO0523.

REFERENCES

1. Shin JW, Kwon SH, Choi JY, et al. Molecular mechanisms of dermal aging and antiaging approaches. *Int J Mol Sci*. 2019;20(9):2126. doi: 10.3390/ijms20092126
2. Meyer PF, de Oliveira P, Silva FKBA, et al. Radiofrequency treatment induces fibroblast growth factor 2 expression and subsequently promotes neocollagenesis and neoangiogenesis in the skin tissue. *Lasers Med Sci*. 2017;32(8):1727-1736. doi: 10.1007/s10103-017-2238-2
3. Maeda-Sano K, Gotoh M, Morohoshi T, Someya T, Murofushi H, Murakami-Murofushi K. Cyclic phosphatidic acid and lysophosphatidic acid induce hyaluronic acid synthesis via CREB transcription factor regulation in human skin fibroblasts. *Biochim Biophys Acta*. 2014;1841(9):1256-1263. doi: 10.1016/j.bbalip.2014.05.004
4. Raab S, Yatskayer M, Lynch S, Manco M, Oresajo C. Clinical evaluation of a multi-modal facial serum that addresses hyaluronic acid levels in skin. *J Drugs Dermatol*. 2017;16(9):884-890.
5. Lee HJ, Seo SR, Yoon MS, Song JY, Lee EY, Lee SE. Microneedle fractional radiofrequency increases epidermal hyaluronan and reverses age-related epidermal dysfunction. *Lasers Surg Med*. 2016;48(2):140-149. doi: 10.1002/lsm.22420
6. Krupkova O, Greutert H, Boos N, Lemcke J, Liebscher T, Wuertz-Kozak K. Expression and activity of hyaluronidases HYAL-1, HYAL-2 and HYAL-3 in the human intervertebral disc. *Eur Spine J*. 2020;29(3):605-615. doi: 10.1007/s00586-019-06227-3
7. Hantash B, Ubeid A, Chang H, Kafi R, Renton B. Bipolar fractional radiofrequency treatment induces neoelastogenesis and neocollagenesis. *Lasers Surg Med*. 2009;41(1):1-9. doi: 10.1002/lsm.20731
8. Narsete T. Evaluation of radiofrequency devices in aesthetic medicine: a preliminary report. *J Dermatol*. 2017;1:5-8.
9. Jewell ML, Solish NJ, Desilets CS. Noninvasive body sculpting technologies with an emphasis on high-intensity focused ultrasound. *Aesthetic Plast Surg*. 2011;35(5):901-912. doi: 10.1007/s00266-011-9700-5
10. Mbeh DA, Hadjab I, Ungur ME, Yahia L. The effect of micropulsatile electrical and ultrasound stimulation on cellular biosynthetic activities such as cellular proliferation, endogenous nitrogen oxide and collagen synthesis. *J Cosmet Dermatol Sci Appl*. 2016;6(1):41-47. doi: 10.4236/jcdsa.2016.61006
11. Bohari SP, Grover LM, Hukins DW. Pulsed low-intensity ultrasound increases proliferation and extracelluar matrix production by human dermal fibroblasts in three-dimensional culture. *J Tissue Eng* 2015;6. 10.1177/2041731415615777
12. Garibyan L, Avashia N. Research techniques made simple: polymerase chain reaction (PCR). *J Invest Dermatol*. 2013;133(3):e6. doi: 10.1038/jid.2013.1
13. Boesl U. Time-of-flight mass spectrometry: introduction to the basics. *Mass Spectrom Rev*. 2017;36(1):86-109. doi: 10.1002/mas.21520
14. Vrioni G, Tsiamis C, Oikonomidis G, Theodoridou K, Kapsimali V, Tsakris A. MALDI-TOF mass spectrometry technology for detecting biomarkers of antimicrobial resistance: current achievements and future perspectives. *Ann Transl Med*. 2018;6(12):240. doi: 10.21037/atm.2018.06.28
15. de la Motte CA, Drazba JA. Viewing hyaluronan. *J Histochem Cytochem*. 2011;59(3):252-257. doi: 10.1369/0022155410397760
16. Heldin P, Basu K, Kozlova I, Porsch H. Chapter eight—HAS2 and CD44 in breast tumorigenesis. In: Simpson MA, Heldin P, eds. *Advances in Cancer Research. Hyaluronan*

Signaling and Turnover. Vol 123. Academic Press; 2014: 211-229. doi:10.1016/B978-0-12-800092-2.00008-3
17. Bourguignon LYW, Ramez M, Gilad E, et al. Hyaluronan–CD44 interaction stimulates keratinocyte differentiation, lamellar body formation/secretion, and permeability barrier homeostasis. *J Invest Dermatol*. 2006;126(6): 1356-1365. doi: 10.1038/sj.jid.5700260
18. Wang Y, Lauer ME, Anand S, Mack JA, Maytin EV. Hyaluronan synthase 2 protects skin fibroblasts against apoptosis induced by environmental stress. *J Biol Chem*. 2014;289(46):32253-32265. doi: 10.1074/jbc.M114.578377
19. Hong L, Shen M, Fang J, et al. Hyaluronic acid (HA)-based hydrogels for full-thickness wound repairing and skin regeneration. *J Mater Sci Mater Med*. 2018;29(9):150. doi: 10.1007/s10856-018-6158-x
20. Horiguchi M, Ota M, Rifkin DB. Matrix control of transforming growth factor-β function. *J Biochem*. 2012;152(4): 321-329. doi: 10.1093/jb/mvs089
21. Hodkovicova N, Hollerova A, Caloudova H, et al. Do foodborne polyethylene microparticles affect the health of rainbow trout (*Oncorhynchus mykiss*)? *Sci Total Environ*. 2021;793:148490. doi: 10.1016/j.scitotenv.2021.148490
22. Lin CY, Kolliopoulos C, Huang CH, et al. High levels of serum hyaluronan is an early predictor of dengue warning signs and perturbs vascular integrity. *EBioMedicine*. 2019;48:425-441. doi: 10.1016/j.ebiom.2019.09.014
23. Citation for the real statistics software or website | real statistics using excel. Accessed December 15, 2021. https://www.real-statistics.com/appendix/citation-real-statistics-software-website/
24. Reed RK, Lilja K, Laurent TC. Hyaluronan in the rat with special reference to the skin. *Acta Physiol Scand*. 1988;134(3): 405-411. doi: 10.1111/j.1748-1716.1988.tb08508.x
25. John HE, Price RD. Perspectives in the selection of hyaluronic acid fillers for facial wrinkles and aging skin. *Patient Prefer Adherence*. 2009;3:225-230. doi: 10.2147/ppa.s3183
26. Reed RK, Laurent UB, Fraser JR, Laurent TC. Removal rate of [3H]hyaluronan injected subcutaneously in rabbits. *Am J Physiol*. 1990;259(2):H532-H535. doi: 10.1152/ajpheart.1990.259.2.H532
27. Papakonstantinou E, Roth M, Karakiulakis G. Hyaluronic acid: a key molecule in skin aging. *Dermatoendocrinology*. 2012;4(3):253-258. doi: 10.4161/derm.21923
28. Fisher GJ, Varani J, Voorhees JJ. Looking older: fibroblast collapse and therapeutic implications. *Arch Dermatol*. 2008;144(5):666-672. doi: 10.1001/archderm.144.5.666
29. Greco RM, Iocono JA, Ehrlich HP. Hyaluronic acid stimulates human fibroblast proliferation within a collagen matrix. *J Cell Physiol*. 1998;177(3):465-473. doi: 10.1002/(SICI)1097-4652(199812)177:3<465::AID-JCP9>3.0.CO;2-5
30. Le T, Ra M, Ej C. Extracellular matrix and dermal fibroblast function in the healing wound. *Adv Wound Care*. 2016;5(3):119-136. doi: 10.1089/Wound.2014.0561
31. Porsch H, Mehić M, Olofsson B, Heldin P, Heldin CH. Platelet-derived growth factor β-receptor, transforming growth factor β type I receptor, and CD44 protein modulate each other's signaling and stability. *J Biol Chem*. 2014;289(28):19747-19757. doi: 10.1074/jbc.M114.547273
32. Torday JS. Homeostasis as the mechanism of evolution. *Biology (Basel)*. 2015;4(3):573-590. doi: 10.3390/biology4030573
33. Han SK, Kim JB, Park H, Lee BI, Kim WK. The effect of hyaluronic acid on fibroblast proliferation in vitro and skin wound healing in vivo. *J Korean Soc Plast Reconstr Surg*. 2002;29(3):211-217.
34. Schlesinger T, Rowland Powell C. Efficacy and safety of a low-molecular weight hyaluronic acid topical gel in the treatment of facial seborrheic dermatitis. *J Clin Aesthet Dermatol*. 2012;5(10):20-23.